Calculation of laminar boundary layers under small harmonic progressive oscillations of the free stream

C. Y. Lam
School of Mechanical & Production Engineering,
Nanyang Technological Institute, Singapore 2263

Received March 1987 and accepted for publication August 1987

This paper describes a method for predicting the response of the two-dimensional, incompressible, laminar boundary layer on a semi-infinite flat plate under small harmonic progressive oscillations of the free-stream velocity for arbitrary frequency and wave speed. The free stream considered consists of a constant mean on which an oscillating amplitude varying with downstream distance is superimposed. The governing equations are solved numerically by a differential-difference technique in conjunction with a series solution for small reduced frequencies. The results are compared with those obtained by other methods and measurements. The results are accurate for a full range of frequency, and the response is very sensitive to changes in the wave convection speed.

Keywords: boundary layer flow; numerical methods; unsteady fluid dynamics

Introduction

Due to technological advances, understanding and predicting unsteady boundary layers in applications such as aircraft in gusts, helicopter rotors in translating motion, and turbomachinery have become more important. However, most existing theoretical[1-7] and experimental[7] investigations have been confined to external flow in which the oscillations are purely time dependent, corresponding to the equation

$$U(x,t)=U_0+U_1\exp(i\omega t)$$

where U, U_0, and U_1 are the instantaneous, mean, and oscillation amplitude of the free-stream velocity, respectively, ω is the radian frequency, x is the streamwise distance, and t is the time. These oscillations convect downstream at infinite wave speed and occur in irrotational flow.

Rotational flow in which harmonic progressive oscillations are induced receives little attention. An example is the vortices shed by a bluff body convecting with a wave speed Q usually less than U_0. The free stream in this type of flow corresponds to

$$U(x,t)=U_0+U_1\exp[i\omega(t-x/Q)]$$

Patel[8-9] presented the boundary layer measurements with free-stream oscillations convecting at a wave speed $Q=0.77U_0$. He also presented approximate theories for low and high frequencies based on the approaches of Lighthill.[1] However, these theories were shown to be erroneous, and a revised high-frequency theory using a different approach was presented in Refs. 10 and 11.

To the author's knowledge, no work has been devoted to solving problems due to harmonic progressive oscillations of the free stream for a full range of frequency and wave speed. The objective of the present work is to devise a method to solve such problems.

Analysis

The usual two-dimensional, incompressible, time-dependent boundary layer equations are

$$\frac{\partial u}{\partial x}+\frac{\partial v}{\partial y}=0 \tag{1}$$

$$\frac{\partial u}{\partial t}+u\frac{\partial u}{\partial x}+v\frac{\partial u}{\partial y}=\frac{\partial U}{\partial t}+U\frac{\partial U}{\partial x}+\nu\frac{\partial^2 u}{\partial y^2} \tag{2}$$

The prescribed free stream containing small harmonic progressive oscillations is

$$U(x,t)=U_0+U_1(x)\exp[i\omega(t-x/Q)] \tag{3}$$

where $U_1(x)\ll U_0$.

Inside the boundary layer, the instantaneous velocity components take the asymptotic expansion form

$$u(x,y,t)=u_0(x,y)+u_1(x,y)\exp[i\omega(t-x/Q)]+\cdots \tag{4a}$$

$$v(x,y,t)=v_0(x,y)+v_1(x,y)\exp[i\omega(t-x/Q)]+\cdots \tag{4b}$$

where $|u_1|\ll|u_0|$ and $|v_1|\ll|v_0|$.

In the limiting case $U_1(x)\ll U_0$, the second and higher harmonic response in (4) can be neglected. Now substitute (3) and (4) into (1) and (2) and extract equal-order amplitude terms. For the mean flow, this gives the usual steady boundary layer equations. For the oscillatory flow, this gives

$$\frac{\partial u_1}{\partial x}-i\omega\frac{u_1}{Q}+\frac{\partial v_1}{\partial y}=0 \tag{5}$$

$$i\omega u_1+u_0\left(\frac{\partial u_1}{\partial x}-i\omega\frac{u_1}{Q}\right)+u_1\frac{\partial u_0}{\partial x}+v_0\frac{\partial u_1}{\partial y}+v_1\frac{\partial u_0}{\partial y}$$
$$=i\omega U_1\left(1-\frac{U_0}{Q}\right)+\nu\frac{\partial^2 u_1}{\partial y^2}+U_0\frac{\mathrm{d}U_1}{\mathrm{d}x} \tag{6}$$

After a rigorous boundary layer analysis,[10] these equations are shown to be valid only when the wavelength of the oscillation is large compared with the mean boundary layer

thickness. We introduce the stream functions ψ_0 and ψ_1 so that

$$u_0=\frac{\partial\psi_0}{\partial y}, \qquad v_0=-\frac{\partial\psi_0}{\partial x}$$

$$u_1=\frac{\partial\psi_1}{\partial y}, \qquad v_1=-\frac{\partial\psi_1}{\partial x}+\frac{i\omega}{Q}\psi_1$$

satisfy the continuity equations (1) and (5), and the transformations

$$\eta=y\left(\frac{U_0}{\nu x}\right)^{1/2}, \quad f_0(\eta)=\frac{\psi_0(x,y)}{(U_0\nu x)^{1/2}}, \quad f_1(x,\eta)=\frac{\psi_1(x,y)}{(U_0\nu x)^{1/2}}$$

The mean flow equation then reduces to the Blasius equation

$$f_0'''+0.5f_0f_0''=0 \tag{7}$$

and the oscillatory flow equation (6) reduces to

$$\frac{\partial^3 f_1}{\partial\eta^3}+\frac{1}{2}\left(f_1f_0''+f_0\frac{\partial^2 f_1}{\partial\eta^2}\right)-i\bar{\omega}\left[\left(1-\frac{U_0}{Q}f_0'\right)\frac{\partial f_1}{\partial\eta}+\frac{U_0}{Q}f_0''f_1-\frac{U_1}{U_0}\left(1-\frac{U_0}{Q}\right)\right]+\frac{x}{U_0}\frac{\mathrm{d}U_1}{\mathrm{d}x}=\bar{\omega}\left(f_0'\frac{\partial^2 f_1}{\partial\bar{\omega}\partial\eta}-f_0''\frac{\partial f_1}{\partial\bar{\omega}}\right) \tag{8}$$

where $\bar{\omega}=\omega x/U_0$ is the reduced frequency and primes denote ordinary differentiation with respect to η. In this equation, $u_0/U_0\equiv f_0'$, $u_1/U_0\equiv\partial f_1/\partial\eta$, and $\bar{\omega}$ has replaced x as the independent variable.

The boundary conditions for (8) are

$$f_1=\frac{\partial f_1}{\partial\eta}=0 \quad \text{at } \eta=0; \qquad \frac{\partial f_1}{\partial\eta}\to\frac{U_1(x)}{U_0} \quad \text{as } \eta\to\infty \tag{9}$$

Numerical procedure

The mean flow is governed by the Blasius equation (7), and the solution f_0, f_0', and f_0'' can easily be obtained by the standard shooting procedure. These f_0-profiles are used in (8) to obtain the solutions for the oscillatory flow.

The governing equation (8) of the oscillatory flow is parabolic and can be solved by marching in the $\bar{\omega}$ (or x) direction with a constant step $\Delta\bar{\omega}$. In general, there will be phase shifts of the boundary layer response with respect to the free stream. Then

$$f_1=f_{1\mathrm{r}}+if_{1\mathrm{i}} \tag{10}$$

where $f_{1\mathrm{r}}$ and $f_{1\mathrm{i}}$ are the real and imaginary components of f_1.

Substituting (10) in (8) and separating real and imaginary parts give

$$\frac{\partial^3 f_{1\mathrm{r}}}{\partial\eta^3}+\frac{1}{2}\left(f_{1\mathrm{r}}f_0''+f_0\frac{\partial^2 f_{1\mathrm{r}}}{\partial\eta^2}\right)+\bar{\omega}\left[\left(1-\frac{U_0}{Q}f_0'\right)\frac{\partial f_{1\mathrm{i}}}{\partial\eta}+\frac{U_0}{Q}f_0''f_{1\mathrm{i}}\right]+\frac{x}{U_0}\frac{\mathrm{d}U_1}{\mathrm{d}x}=\bar{\omega}\left(f_0'\frac{\partial^2 f_{1\mathrm{r}}}{\partial\bar{\omega}\partial\eta}-f_0''\frac{\partial f_{1\mathrm{r}}}{\partial\bar{\omega}}\right) \tag{11a}$$

$$\frac{\partial^3 f_{1\mathrm{i}}}{\partial\eta^3}+\frac{1}{2}\left(f_{1\mathrm{i}}f_0''+f_0\frac{\partial^2 f_{1\mathrm{i}}}{\partial\eta^2}\right)-\bar{\omega}\left[\left(1-\frac{U_0}{Q}f_0'\right)\frac{\partial f_{1\mathrm{r}}}{\partial\eta}+\frac{U_0}{Q}f_0''f_{1\mathrm{r}}-\frac{U_1}{U_0}\left(1-\frac{U_0}{Q}\right)\right]=\bar{\omega}\left(f_0'\frac{\partial^2 f_{1\mathrm{i}}}{\partial\bar{\omega}\partial\eta}-f_0''\frac{\partial f_{1\mathrm{i}}}{\partial\bar{\omega}}\right) \tag{11b}$$

The boundary conditions (9) now become

$$f_{1\mathrm{r}}=f_{1\mathrm{i}}=\frac{\partial f_{1\mathrm{r}}}{\partial\eta}=\frac{\partial f_{1\mathrm{i}}}{\partial\eta}=0 \quad \text{at } \eta=0$$

$$\frac{\partial f_{1\mathrm{r}}}{\partial\eta}\to\frac{U_1(x)}{U_0}, \quad \frac{\partial f_{1\mathrm{i}}}{\partial\eta}\to 0 \quad \text{as } \eta\to\infty \tag{12}$$

Using three-point backward finite difference representations for the $\bar{\omega}$-derivative terms—for example,

$$\left[\frac{\partial f_{1\mathrm{r}}}{\partial\bar{\omega}}\right]^n=\frac{1.5f_{1\mathrm{r}}^n-2f_{1\mathrm{r}}^{n-1}+0.5f_{1\mathrm{r}}^{n-2}}{\Delta\bar{\omega}}$$

where the superscripts denote streamwise station numbers—we reduce the pair of third-order coupled linear partial differential equations (11) to ordinary differential equations. The resulting equations are then replaced by a system of first-order equations:

$$f_{\mathrm{r}}'=u_{\mathrm{r}}$$

$$u_{\mathrm{r}}'=v_{\mathrm{r}}$$

$$v_{\mathrm{r}}'=-0.5(f_{\mathrm{r}}f_0''+f_0v_{\mathrm{r}})-\frac{1.5\bar{\omega}}{\Delta\bar{\omega}}(f_{\mathrm{r}}f_0''-f_0'u_{\mathrm{r}})-\bar{\omega}\left[\left(1-\frac{U_0}{Q}f_0'\right)u_{\mathrm{i}}+\frac{U_0}{Q}f_0''f_{\mathrm{i}}\right]-\frac{x}{U_0}\frac{\mathrm{d}U_1}{\mathrm{d}x}+\frac{\bar{\omega}}{\Delta\bar{\omega}}[f_0'(0.5u_{\mathrm{r}}^{n-2}-2u_{\mathrm{r}}^{n-1})-f_0''(0.5f_{\mathrm{r}}^{n-2}-2f_{\mathrm{r}}^{n-1})] \tag{13a}$$

Notation

U	Free-stream velocity
x, y	Boundary layer coordinates
u, v	Velocity components in the x- and y-directions, respectively
t	Time coordinate
ψ	Stream function
f	Dimensionless stream function
η	Dimensionless coordinate in the y-direction
ω	Radian frequency
Q	Wave convection speed
λ	Wavelength
ν	Kinematic viscosity
$\bar{\omega}$	Dimensionless frequency parameter
ϕ	Velocity phase angle
ρ	Density of the fluid
p	Pressure
τ	Shear stress

Subscripts

∞	Ambient conditions
w	Wall conditions
0	Mean components
1	Oscillatory components
r	Real components
i	Imaginary components

$$f_i' = u_i$$

$$u_i' = v_i$$

$$v_i' = -0.5(f_i f_0'' + f_0 v_i) - \frac{1.5\bar{\omega}}{\Delta\bar{\omega}}(f_i f_0'' - f_0' u_i) + \bar{\omega}\left[\left(1-\frac{U_0}{Q}f_0'\right)u_r + \frac{U_0}{Q}f_0'' f_r - \frac{U_1}{U_0}\left(1-\frac{U_0}{Q}\right)\right] + \frac{\bar{\omega}}{\Delta\bar{\omega}}\left[f_0'(0.5u_i^{n-2} - 2u_i^{n-1}) - f_0''(0.5f_i^{n-2} - 2f_i^{n-1})\right] \quad (13b)$$

where $(f_r, u_r, v_r, f_i, u_i, v_i) \equiv (f_{1r}, f_{1r}', f_{1r}'', f_{1i}, f_{1i}', f_{1i}'')$ and the superscript n is dropped. The boundary conditions are

$$f_r = u_r = f_i = u_i = 0 \quad \text{at } \eta = 0$$

$$u_r \to \frac{U_1(x)}{U_0}, \quad u_i \to 0 \quad \text{as } \eta \to \infty \quad (14)$$

Assuming that the solutions at the $(n-1)$st and $(n-2)$nd stations have been obtained and that the unknowns f_i and u_i in (13a) take the values at the $(n-1)$st station as their first iterates, we can solve (13a) by a "multisuperposition" method (described later). Using f_r and u_r so obtained as their first iterates in (13b), we can solve this equation by the same superposition method to get the second iterates of f_i and u_i. The iteration is repeated until the following convergence criterion is satisfied at nine preselected η-points across the boundary layer thickness:

$$\left|\frac{u_{r_{k+1}} - u_{r_k}}{u_{r_k}}\right| \leqq 10^{-3} \quad \text{and} \quad \left|\frac{u_{i_{k+1}} - u_{i_k}}{(u_{i_k})_{max}}\right| \leqq 10^{-3}$$

where k and $k+1$ denote iterate numbers.

After obtaining a solution, we can march in the $\bar{\omega}$-direction to generate solutions at different $\bar{\omega}$ values.

The series solution

To start the above iterative procedure, we need solutions at the first (i.e., leading edge) and second stations, where x is small or $\bar{\omega} \ll 1$. These solutions are obtained by series of the form

$$f_{1r}(\bar{\omega}, \eta) = \sum_{j=0}^{5} G_j(\eta)\bar{\omega}^j \quad (15a)$$

$$f_{1i}(\bar{\omega}, \eta) = \sum_{j=0}^{5} H_j(\eta)\bar{\omega}^j \quad (15b)$$

Equations 15a and 15b are actually series expansions in streamwise distance x rather than $\bar{\omega}$. To obtain the series solution, we need the U_1 variation with x. In previous investigations,[1-9] U_1 was either constant or varied linearly with x. The present work thus assumes

$$U_1(x) = C_0 + C_1 x \quad (16)$$

where C_0 and C_1 are prescribed constants. Equation 16 remains valid for general distribution of U_1 to first-order approximation when x is small. Substituting (15) and (16) into (11) and grouping terms of the same order give,

$$G_0''' + 0.5f_0G_0'' + 0.5f_0''G_0 = 0$$
$$H''' + 0.5f_0H_0'' + 0.5f_0'' = 0 \quad \text{for } \bar{\omega}^0 \text{ terms} \quad (17a)$$

$$G_1''' + 0.5f_0G_1'' - f_0'G_1' + 1.5f_0''G_1 + H_0'\left(1-\frac{U_0}{Q}f_0'\right) + \frac{U_0}{Q}f_0''H_0 + \frac{C_1}{\omega} = 0$$
$$H_1''' + 0.5f_0H_1'' - f_0'H_1' + 1.5f_0''H_1 \quad \text{for } \bar{\omega}^1 \text{ terms} \quad (17b)$$

$$-G_0'\left(1-\frac{U_0}{Q}f_0'\right) - \frac{U_0}{Q}f_0''G_0 + \frac{C_0}{U_0}\left(1-\frac{U_0}{Q}\right) = 0$$

$$G_2''' + 0.5f_0G_2'' - 2f_0'G_2' + 2.5f_0''G_2 + H_1'\left(1-\frac{U_0}{Q}f_0'\right) + \frac{U_0}{Q}f_0''H_1 = 0$$
$$H_2''' + 0.5f_0H_2'' - 2f_0'H_2' + 2.5f_0''H_2 \quad \text{for } \bar{\omega}^2 \text{ terms} \quad (17c)$$

$$-G_1'\left(1-\frac{U_0}{Q}f_0'\right) - \frac{U_0}{Q}f_0''G_1 + \frac{C_1}{\omega}\left(1-\frac{U_0}{Q}\right) = 0$$

$$G_n''' + 0.5f_0G_n'' - nf_0'G_n' + (n+0.5)f_0''G_n + H_{n-1}'\left(1-\frac{U_0}{Q}f_0'\right) + \frac{U_0}{Q}f_0''H_{n-1} = 0$$
$$\text{for } \bar{\omega}^n \ (n = 3, 4, 5) \text{ terms} \quad (17d)$$

$$H_n''' + 0.5f_0H_n'' - nf_0'H_n' + (n+0.5)f_0''H_n - G_{n-1}'\left(1-\frac{U_0}{Q}f_0'\right) - \frac{U_0}{Q}f_0''G_{n-1} = 0$$

The boundary conditions are

$$\text{at } \eta = 0, \quad G_n = H_n = G_n' = H_n' = 0 \quad \text{for } n = 0, 1, \ldots, 5$$

$$\text{as } \eta \to \infty, \quad G_0' = \frac{C_0}{U_0}, \quad G_1 = \frac{C_1}{\omega}, \quad G_2' = G_3' = G_4' = G_5' = 0 \quad (18)$$

$$H_n' = 0 \quad \text{for } n = 0, 1, \ldots, 5$$

The above sets of linear ordinary differential equations are solved successively by the standard superposition method without any special treatment.

The solution at the leading edge is

$$f_{1r}(0, \eta) = G_0(\eta), \qquad f_{1i}(0, \eta) = H_0(\eta)$$

and the solution at the second station is

$$f_{1r}(\Delta\bar{\omega}, \eta) = \sum_{j=0}^{5} G_j(\eta)(\Delta\bar{\omega})^j, \qquad f_{1i}(\Delta\bar{\omega}, \eta) = \sum_{j=0}^{5} H_j(\eta)(\Delta\bar{\omega})^j$$

Multisuperposition method

At far downstream distances, $\bar{\omega}/\Delta\bar{\omega}$ $(\equiv x/\Delta x)$ in (13) becomes very large. The complementary function and the particular integral therefore grow rapidly, causing an overflow problem in the computation before integration reaches the boundary layer edge. The multisuperposition method is used to overcome this difficulty.

To prevent the overflow problem, we use a small initial value for $v_r(\bar{\omega}, 0) = 10^{-40}$ for the complementary function. For the particular integral, we construct a function $u_r(\bar{\omega}, \eta) = u_{rg}(\bar{\omega}, \eta)$, say, by stretching the $u_r(\bar{\omega}, \eta)$ profile at the previous station so that u_{rg} satisfies the outer condition $u_{rg}(\bar{\omega}, \eta_\infty) = U_1(x)/U_0$. The integration stops when u_r of the particular integral exceeds 10^3 at $\eta = \eta_1$. Then the standard superposition is done from $\eta = 0$ to $n = \eta_1$, so the superimposed solution satisfies $u_r(\bar{\omega}, \eta_1) = u_{rg}(\bar{\omega}, \eta_1)$. Using $f_r(\bar{\omega}, \eta_1)$, $u_r(\bar{\omega}, \eta_1)$, and $v_r(\bar{\omega}, \eta_1)$ as initial values, we resume integration from η_1 outward until u_r exceeds 10^3 at η_2. The superposition is done again from $\eta = \eta_1$ to $\eta = \eta_2$, so $u_r(\bar{\omega}, \eta_2) = u_{rg}(\bar{\omega}, \eta_2)$. These steps are repeated until η_∞ is reached. The final superimposed solution is the required solution.

The same multisuperposition method is applied to (13b) for the imaginary part of the oscillatory flow. In this case, the function $u_{ig}(\bar{\omega}, \eta)$ required to obtain the particular integral is taken to be $u_i(\bar{\omega}, \eta)$ at the previous station.

Throughout the computation, $\eta_\infty = 9$, $\Delta\eta = 0.1$, and

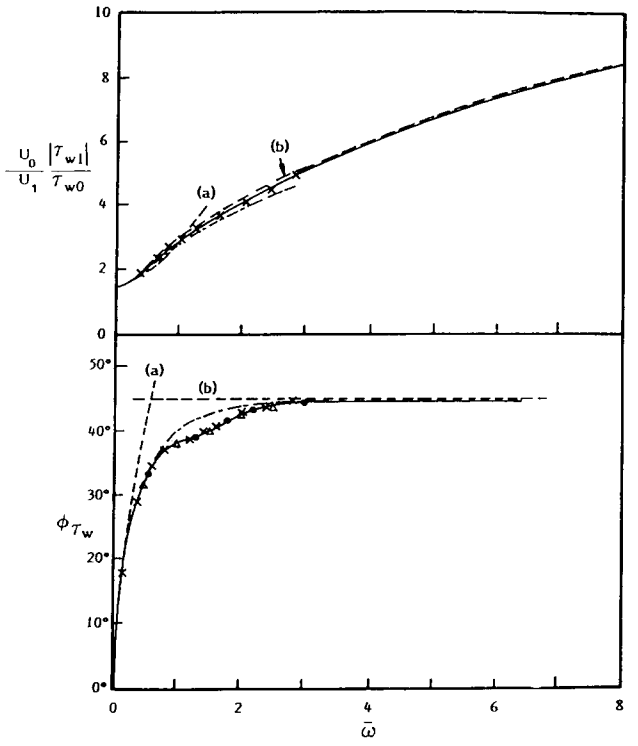

Figure 1 Variations of amplitude and phase of wall shear from different theories ($Q\to\infty$): —— present; – – – – Lighthill[1], (a) low- and (b) high-frequency results; △, Ackerberg and Phillips[2]; — — — McCroskey and Philippe[3]; × Cebeci[4]; ● Telionis and Romaniuk[5]

$\Delta\bar{\omega}=0.1\omega/U_0$ are used. All integrations are done by the fourth-order Runge-Kutta method.

Results

In terms of the transformed variables, the oscillatory velocity-amplitude ratio $|u_1|/U_1$ and the phase angle ϕ between u_1 and the free-stream velocity are

$$\frac{|u_1|}{U_1}=\frac{U_0}{U_1}\left[\left(\frac{\partial f_{1r}}{\partial\eta}\right)^2+\left(\frac{\partial f_{1i}}{\partial\eta}\right)^2\right]^{1/2} \tag{19a}$$

and

$$\phi=\tan^{-1}\left[\frac{\partial f_{1i}/\partial\eta}{\partial f_{1r}/\partial\eta}\right] \tag{19b}$$

At the wall, the velocity phase angle is

$$\phi_{\eta\to 0}=\lim_{\eta\to 0}\phi=\tan^{-1}\left[\frac{\partial^2 f_{1i}/\partial\eta^2}{\partial^2 f_{1r}/\partial\eta^2}\right] \tag{19c}$$

Similar to other boundary layer parameters, the wall shear stress τ_w consists of a mean τ_{w0} and an oscillatory τ_{w1} component; that is,

$$\tau_w=\tau_{w0}+\tau_{w1}\exp[i\omega(t-x/Q)]$$

In this expression, $\tau_{w1}=\tau_{w1r}+i\tau_{w1i}$, where τ_{w1r} and τ_{w1i} are the real and imaginary part, respectively. The wall shear amplitude ratio $|\tau_{w1}|/\tau_{w0}$ and the phase angle ϕ_{τ_w} between the wall shear and the free stream are

$$\frac{|\tau_{w1}|}{\tau_{w0}}=\left[\frac{\partial u_1/\partial y|}{\partial u_0/\partial y}\right]_{y=0}=\left\{\frac{[(\partial^2 f_{1r}/\partial\eta^2)^2+(\partial^2 f_{1i}/\partial\eta^2)^2]^{1/2}}{d^2 f_0/d\eta^2}\right\}_{\eta=0} \tag{20a}$$

and

$$\phi_{\tau_w}=\tan^{-1}\left[\frac{\partial^2 f_{1i}/\partial\eta^2}{\partial^2 f_{1r}/\partial\eta^2}\right]_{\eta=0} \tag{20b}$$

Equations 19 and 20 are used to compute the respective quantities $|u_1|/U_1$, ϕ, $\phi_{\eta\to 0}$, $|\tau_{w1}|/\tau_{w0}$, and ϕ_{τ_w}.

Limiting case $Q\to\infty$

This case has been studied extensively by many researchers, both theoretically[1–7] and experimentally.[7] It provides a useful test case to validate the present computation. These studies assumed constant U_0 and U_1. Figure 1 displays the comparison of the amplitude and phase of wall shear from the present method with those from various existing theories.[1–5] Excellent agreement is obvious from low to high reduced frequencies. In Figures 2–4, the velocity amplitude ratio and the velocity phase angle for a wide range of $\bar{\omega}$ are compared with the theoretical results of Farn and Arpaci[6] and the experimental results of Hill and Stenning.[7] Again, excellent agreement is obtained.

Finite wave speed Q

The experimental results suitable for comparison are obtained from Patel,[8–9] His measurements were made at $x=0.25$ m with $U_0=10\,\mathrm{m\,s^{-1}}$, $U_1=(0.449+0.468x)\,\mathrm{m\,s^{-1}}$, and $Q=0.77U_0$. These values are used in the present computation, and the results for velocity amplitude ratio and velocity phase angle are plotted in Figure 5 together with the measurements for $\bar{\omega}=0.314$ and 1.257. The agreement is poor. Recent measurements[12] using the same experimental facilities as used by Patel[9] verify that Q decreases with downstream distance and that $Q\simeq 0.61U_0$ at Patel's measuring station, where $x=0.25$ m. Figure 6 displays the results for $Q=0.61U_0$ and $\bar{\omega}=0.314$, 0.628, 1.257, and 1.571. It shows significant improvement in the agreement with the measurements. The phase angle profiles are accurately predicted. The computed velocity ratio profiles agree well with the measurements and clearly exhibit large overshoots and dips at high reduced frequencies. For the

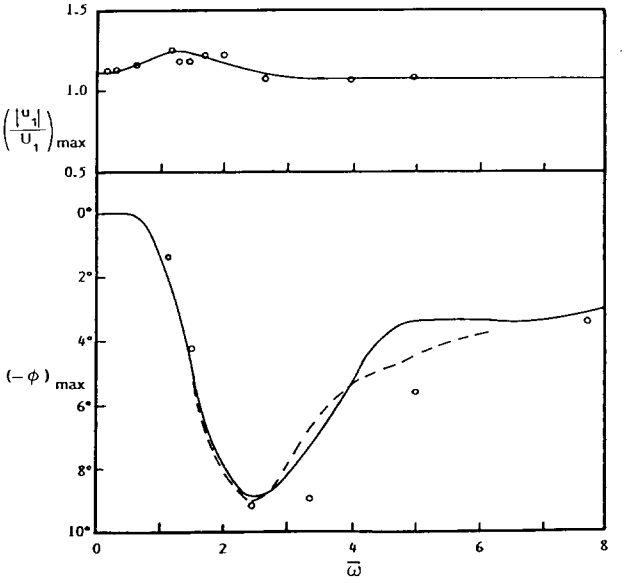

Figure 2 Variations of maximum velocity ratio and phase lag ($Q\to\infty$): —— present theory; – – – theory, Farn and Arpaci[6]; ○ experiment, Hill and Stenning[7]

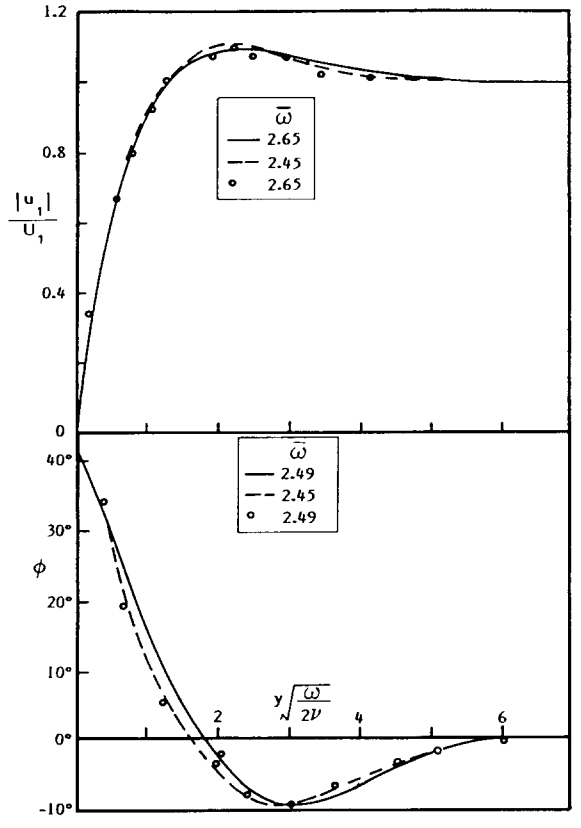

Figure 3 Oscillating boundary layer profiles ($Q\to\infty$): ——— present; – – – theory, Farn and Arpaci[6]; ○ experiment, Hill and Stenning[7]

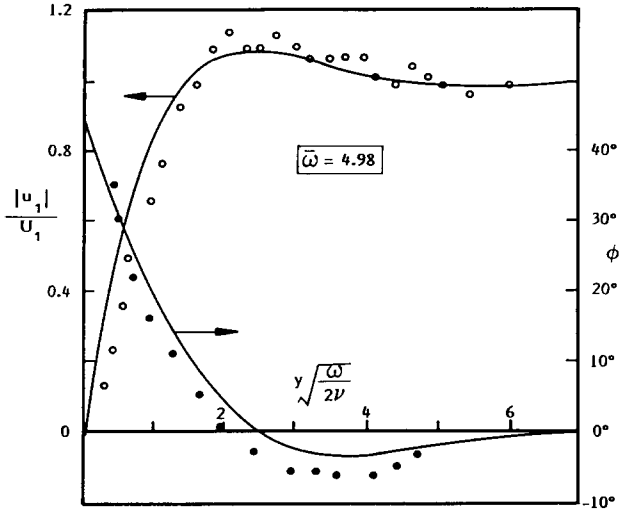

Figure 4 Oscillating boundary layer profiles ($Q\to\infty$): —— present; ○ ● experiment, Hill and Stenning[7]

frequencies used in the computation, the velocity overshoot increases and shifts closer to the wall as frequency increases. At high frequency, velocity dip occurs in the outer region of the boundary layer, and it also increases with the frequency. Throughout the boundary layer, the velocity phase lag increases with frequency.

The effects of convection wave speed Q on the boundary layer response are shown in Figures 7 and 8 for velocity amplitude ratio profile and velocity phase angle profile, respectively. The results in these figures are obtained for $x=0.25$ m, $U_0=10\ \mathrm{m\,s^{-1}}$, $U_1=(0.449+0.468x)\ \mathrm{m\,s^{-1}}$, and $\bar{\omega}=1.571$. From the velocity ratio plots, velocity dips and huge velocity overshoots occur for small values of Q/U_0. As Q/U_0 increases from a small value, the overshoot decreases and the velocity dip increases. Eventually, the overshoot and dip disappear at $Q/U_0=1$, and the velocity ratio increases with η in a gradual monotonic manner. As Q/U_0 increases further, the overshoot reappears and tends to an asymptotic value of 1.24 as $Q/U_0\to\infty$. The velocity profile is highly sensitive to Q/U_0 for $Q/U_0<1$. From the phase angle plots, the velocity inside the entire boundary layer lags the free-stream velocity for small Q/U_0. As Q/U_0 increases, the phase angle increases. Eventually, the velocity in the inner part of the boundary layer leads the free stream while that in the outer part lags.

Discussion

The present method is developed for free-stream oscillations with wide ranges of wave convection speed and frequency. The requirements are that the oscillation amplitude must be small compared with the mean flow speed and that the wavelength λ of the oscillation must be large compared with the mean boundary layer thickness. Since $\lambda=2\pi Q/\omega$, the wave speed cannot be too small and the frequency cannot be too large in order to meet the latter requirement. However, the wave speed and the frequency rarely fall into these extremes.

The results of the method agree well with available measurements and the results obtained by other methods. In addition, it is found that the series solution and the differential-difference solution for small reduced frequencies are almost identical.

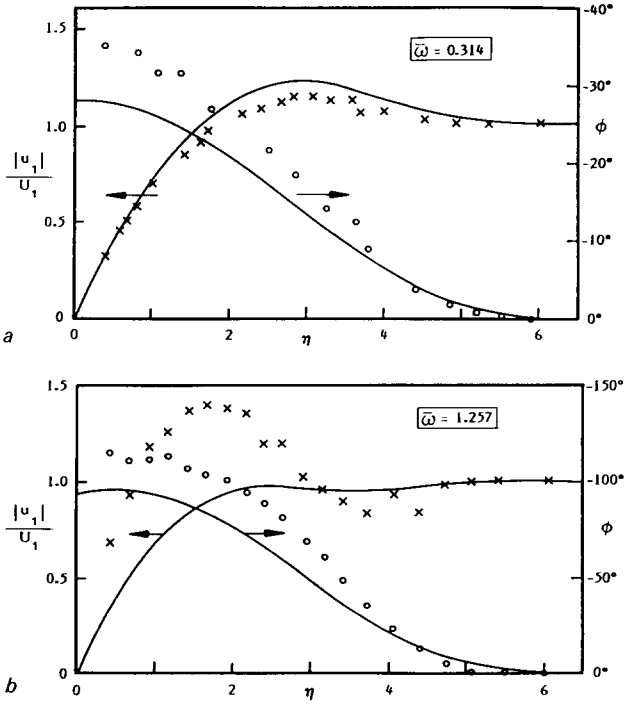

Figure 5 Oscillating boundary layer profiles ($Q=0.77U_0$): —— present; × ○ experiment, Patel[9]

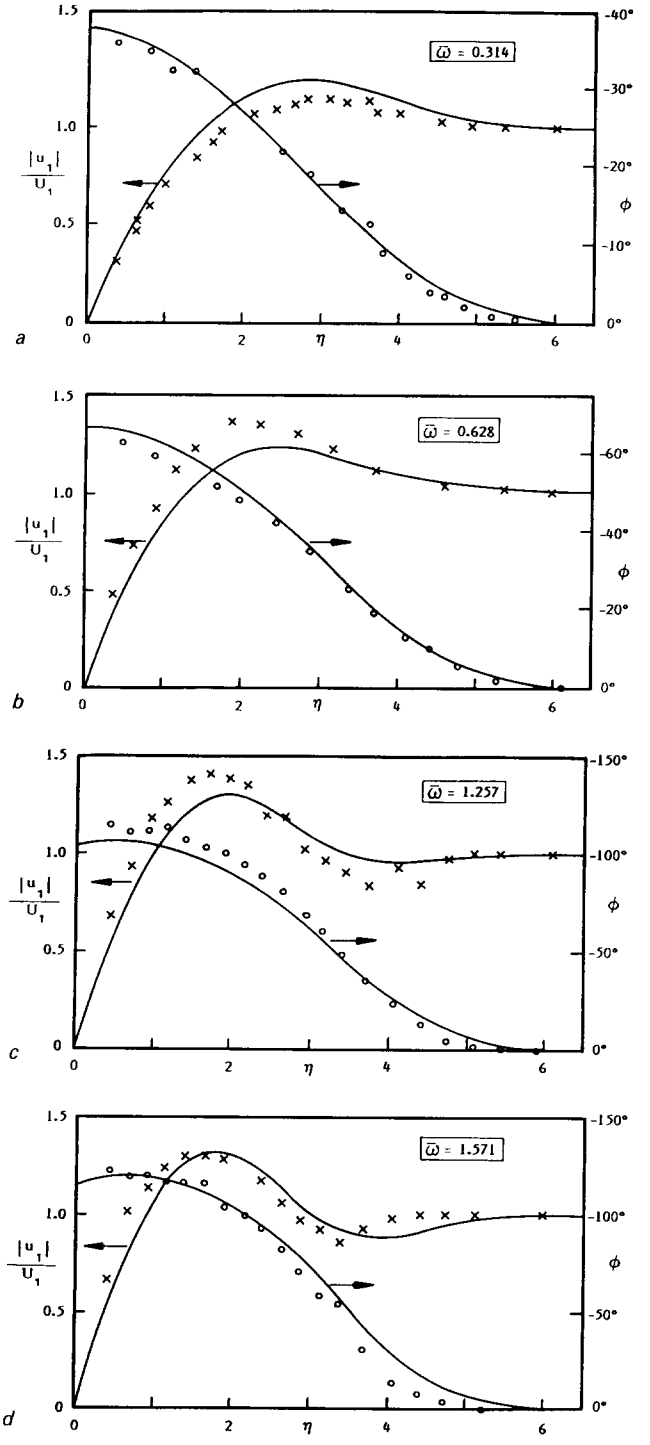

Figure 6 Oscillating boundary layer profiles: —— present, $Q=0.61U_0$; × ○ experiment, $Q=0.77U_0$ (nominal), Patel[9]

Further, some solutions of the method were compared with those of the revised high-frequency theory for finite wave speed in Ref. 11 and good agreement was obtained. Based on these, it may be concluded that the present method is accurate.

The analysis yields a mean flow boundary layer equation (7) identical to the steady flow equation. This implies that the mean flow is unaffected by the free-stream unsteadiness, which has been confirmed by various experiments.[7–9]

The boundary layer shows entirely different response for $Q/U_0<1$ and $Q/U_0>1$, as illustrated in Figures 7 and 8, because the free-stream oscillating pressure gradient

$$\frac{\partial p}{\partial x}=-\rho\left(\frac{\partial U}{\partial t}+U\frac{\partial U}{\partial x}\right)$$
$$=i\omega\rho u_1\left(\frac{U_0}{Q}-1\right)\exp\left[i\omega\left(t-\frac{x}{Q}\right)\right],$$

where p and ρ are pressure and density, respectively, that drives the boundary layer has different signs for the two cases. Furthermore, the quantity $(U_0/Q-1)$ is more sensitive to

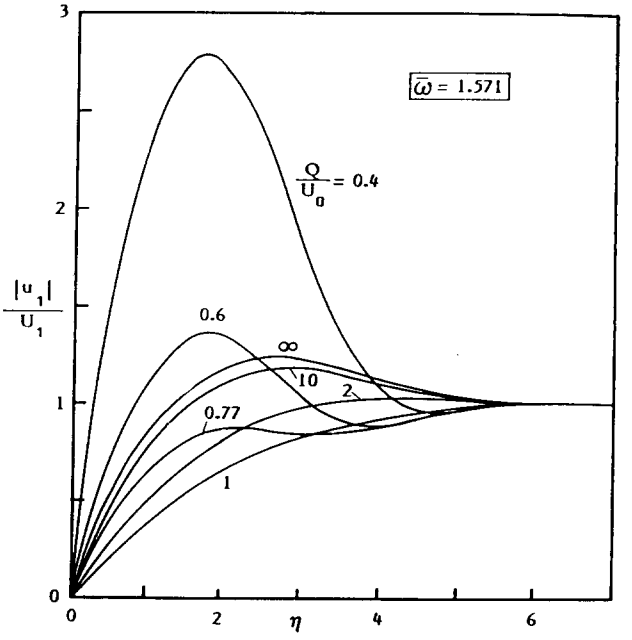

Figure 7 Velocity ratio profiles for different Q/U_0

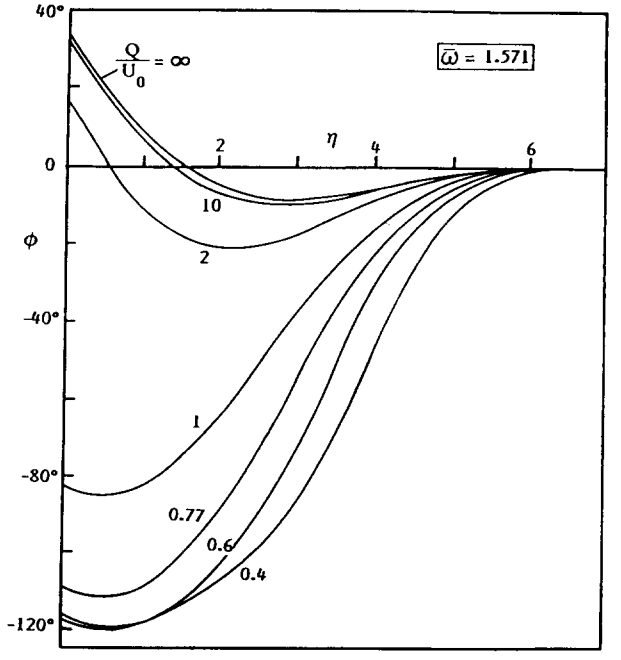

Figure 8 Velocity phase angle profiles for different Q/U_0

changes in Q/U_0 for $Q/U_0<1$ than for $Q/U_0>1$. This is illustrated as follows:

Q/U_0	0.4	0.6	0.8	1.0	1.2	1.4	1.6
$(U_0/Q-1)$	1.50	0.67	0.25	0	−0.17	−0.29	−0.38

This means that the change in the free-stream pressure gradient is larger for $Q/U_0<1$ than for $Q/U_0>1$. Consequently, when Q/U_0 is small, the response is sensitive to changes in Q/U_0, which can be clearly seen in Figures 7 and 8. For this reason, the value of the wave speed should be carefully measured in future experiments with similar conditions.

Conclusions

A method is presented for predicting the response of the two-dimensional, incompressible laminar boundary layer under small harmonic progressive free-stream oscillations. The main feature of the method is its ability to deal with full ranges of free-stream oscillation frequency and wave speed. Extensive comparison of the present results with those obtained by other methods and measurements shows that the method is accurate. It is also found that the wave speed, when less than the mean free-stream speed, is sensitive to the boundary layer response.

References

1 Lighthill, M. J. The response of laminar skin friction and heat transfer to fluctuations in the stream velocity. *Proc. Roy. Soc. Lond.*, 1954, **A224**, 1

2 Ackerberg, R. C. and Phillips, J. H. The unsteady laminar boundary layer on a semi-infinite flat plate due to small fluctuations in the magnitude of the free-stream velocity. *J. Fluid Mech.*, 1972, **51**, 137

3 McCroskey, W. J. and Philippe, J. J. Unsteady viscous flow on oscillating airfoils. *AIAA J.*, 1975, **13**, 71

4 Cebeci, T. Calculation of unsteady two-dimensional laminar and turbulent boundary layers with fluctuations in external velocity. *Proc. Roy. Soc. Lond.*, 1977, **A355**, 225

5 Telionis, D. P. and Romaniuk, M. S. Velocity and temperature streaming in oscillating boundary layers. *AIAA J.*, 1978, **16**, 488

6 Farn, C. L. S. and Arpaci, V. S. On the numerical solution of unsteady laminar boundary layers. *AIAA J.*, 1966, **4**, 730

7 Hill, P. G. and Stenning, A. H. Laminar boundary layers in oscillatory flow. *ASME J. Basic Engrg.*, 1960, **82D**, 593

8 Patel, M. H. On unsteady boundary layers. Ph.D. Thesis, Univ. of London, 1974

9 Patel, M. H. On laminar boundary layers in oscillatory flow. *Proc. Roy. Soc. Lond.*, 1975, **A347**, 99

10 Lam, C. Y. Unsteady laminar and turbulent boundary layer computations using a differential-difference method. Ph.D. Thesis, Univ. of London, 1983

11 Horton, H. P. and Lam, C. Y. The response of laminar boundary layers to small progressive oscillations of the free-stream velocity. Proc. 3rd Int. Conf. on Boundary and Interior Layers, 1984, 232

12 Horton, H. P. Private communication, 1984